Pergamon

Cement and Concrete Research 29 (1999) 1331–1340

CEMENT AND CONCRETE RESEARCH

Thaumasite formation in Portland-limestone cement pastes

S.A. Hartshorn, J.H. Sharp*, R.N. Swamy

Centre for Cement and Concrete and Department of Engineering Materials, The University of Sheffield, Mappin Street, Sheffield, England S1 3JD, UK

Received 17 September 1998; accepted 27 April 1999

Abstract

Small cylinders (10-mm diameter × 10-mm height) made at a water:solids ratio of 0.5 from Portland cement with 0, 5, 15, and 30% limestone additions were cured in water at room temperature for 28 days. They were subsequently stored in various solutions at 5°C for periods of up to 420 days. The pastes were inspected visually and examined by X-ray diffraction every 28 days. Selected samples were also examined by thermal analysis and scanning electron microscopy. Pastes containing fine limestone additions were susceptible to formation of thaumasite after only a few months of exposure to sulfate solutions. The extent of thaumasite formation was greater with increasing limestone additions and when magnesium sulfate was present in the solution. Thaumasite formation was then accompanied by formation of brucite and secondary gypsum. Calcium hydroxide was a reactant rather than a reaction product and C-S-H gel was also consumed.

Keywords: X-ray diffraction; Durability; Sulfate attack; Portland-limestone cement; Thaumasite

1. Introduction

A recent report [1] highlighted the identification of thaumasite as a product of sulfate attack of columns supporting bridges over a motorway in southwest England. These structures were made using both ordinary and sulfate-resisting Portland cement, yet excavation has revealed that in places the concrete cover had been eroded down to the reinforcement. Thaumasite is a complex hydrate with the formula $CaSiO_3 \cdot CaCO_3 \cdot CaSO_4 \cdot 15H_2O$, or in cement chemists' notation, $C_3S\overline{C}\overline{S}H_{15}$. It is believed to form in cool, damp conditions when groundwater containing sulfate ions comes into contact with Portland cement and limestone aggregate.

The use of limestone aggregates has been common in the United Kingdom and elsewhere for many decades. Indeed, in recent years it has become common practice to incorporate fine limestone dust as a minor additional constituent in the cement paste, whether or not a coarse limestone aggregate is also used to make concrete. The European standard allows the use of the term "ordinary Portland cement" with incorporation of up to 5% or less limestone, while the term "Portland-limestone cement" is used for cements containing 5–35% limestone replacement of Portland cement. It seemed timely, therefore, to investigate the hydration of a range of cement pastes with 0–35% limestone replacement under conditions that might lead to the formation of thaumasite.

More specifically, the objectives of the present study were to identify potential durability problems associated with limestone-filled cements, to assess the effect of limestone fillers on sulfate resistance, and to compare the rate of deterioration of cement pastes in the presence of $MgSO_4$, Na_2SO_4, and mixtures of the two.

2. Experimental

Ordinary Portland cement (OPC) was provided by Castle Cement Ltd. (Ribblesdale, England) and was of typical composition, as shown in Table 1. From a conventional Bogue calculation, the potential phase composition was C_3S, 48.7; C_2S, 23.7; C_3A, 8.5; and C_4AF, 9.1. The limestone used was a carboniferous limestone from the north of England, with a calcium carbonate content of >98%. The full analysis is shown in Table 1.

Cement paste cylinders were prepared and stored in various solutions as shown in Table 2. Mixing and casting of the cement paste was carried out in batches of 104 cylinders, using approximately 200 g of cement (with added limestone as appropriate) and 100 g of water (for a water:solids ratio of 0.5, which was used unless specified). The cement and ground limestone were blended prior to mixing. The pastes were hand-mixed and the water was added gradually. After all the water had been incorporated in the mix, a further 3

* Corresponding author. Tel.: +44-114-222-5501; fax: +44-114-222-5943.

E-mail address: j.h.sharp@sheffield.ac.uk (J.H. Sharp)

0008-8846/99/$ – see front matter
PII: S0008-8846(99)00100-3

Table 1
Chemical analyses of Portland cement and ground limestone

Component	Weight (%)	
	OPC	Limestone
SiO_2	21.1	0.86
Al_2O_3	5.1	0.08
Fe_2O_3	3.0	0.34
CaO	64.6	56.3
MgO	2.9	0.58
SO_3	2.9	–
K_2O	0.7	0.05
Na_2O	0.3	0.08
Loss on ignition	0.2	42.0
Free lime	1.7	–
Total	100.8	100.29

Table 2
Mix design and storage conditions for cement paste cylinders

Cylinder size	10 mm diameter × 10 mm
Water/cement ratio	0.4, 0.5, 0.75
Storage temperature	5, 10, 15°C
Limestone additions	0, 5, 15, 35%
Storage conditions	A, boiled tap water
	B, distilled water
	C, 0.4% $MgSO_4$
	D, 1.8% $MgSO_4$
	E, 0.4% Na_2SO_4
	F, 1.8% Na_2SO_4
	G, 0.4% $MgSO_4$ + 0.4% Na_2SO_4
	H, 1.8% $MgSO_4$ + 1.8% Na_2SO_4

min of mixing was undertaken. The paste was poured into PTFE moulds and tamped with a glass rod. Efforts were made to expel any remaining air bubbles. The moulds were covered with polythene sheeting and air cured for 24 h before demoulding. The cylinders were then transferred to plastic beakers and water-cured for a further 27 days at room temperature (approximately 20°C). After this initial period of hydration, the cylinders were transferred to labelled test tubes with a diameter of 14 mm that contained pre-chilled solutions of the correct concentration, and stored in a water bath at 5°C. The cylinders were totally immersed in the solutions, which were changed every 3 months (84 days).

After storage for successive periods of 28 days, selected cylinders were crushed and then ground by hand, using acetone as a grinding aid to halt the hydration of the paste. The samples were ground to pass a 53-μm sieve and then dried for 2 h in a vacuum desiccator. The dried powder was loaded into a backfill sample holder to reduce effects caused by preferred orientation of platy or acicular crystals. X-ray analysis was carried out using copper radiation on a Philips 1710 diffractometer (Philips, Holland) in conjunction with SIE 1770 and Traces software (Sietronics Ply Ltd., Belconnen, Australia). Initially a range from 5 to 65° 2θ and a scanning speed of 2° 2θ were used, but to scan effectively the more important range at lower angles, scanning speeds of 1° 2θ and 0.5° 2θ were also used. The slower scanning speeds did not produce significantly better resolution.

X-ray diffraction (XRD) traces of some standards were obtained to compare the phases identified in the test specimens with pure minerals and/or synthetic phases. The most important of these was a mineral sample of thaumasite from Crestmore, California, USA, and a synthetic sample of ettringite from the British Cement Association (courtesy of Mr. W. Gutteridge).

Differential scanning calorimetry (DSC) was carried out on selected deteriorated cement pastes and some standard materials using a Du Pont TA 2000 differential scanning calorimeter. Dried powder (10 mg) was weighed into an aluminum sample holder and heated from room temperature to 600°C at 10°C/min in a flowing atmosphere of nitrogen.

Scanning electron microscopy (SEM) was carried out on selected samples to assess their mineralogy and microstructure. Some polished sections of deteriorated samples were made, but due to the porous nature of the reaction surface it was difficult to achieve a well-polished surface. Most of the SEM was direct observation of deteriorated surfaces and fracture surfaces using stub samples. For such samples, small pieces of cement paste were dried in a vacuum desiccator for 3 days. They were sputter coated with a gold coating and examined on a CamScan (Cambridge Instruments, Cambridge, England) electron microscope with energy-dispersive X-ray analysis using Link software (Link Analytical, High Wycombe, England). The accelerating voltage was 20 kV and the stub samples were examined by secondary electron imaging.

3. Results

3.1. Visual inspection

A visual inspection of the cylinders was carried out on a monthly basis to assess any visible changes and to link any such changes to variation in mineralogy and microstructure.

The neat Portland cement pastes were quite resistant to the sulfate-containing solutions, even at high concentrations, for up to 252 days. Beyond this period, the edges and surface of the cylinders started to spall. The two cylinders that were affected the worst were those stored in solutions D and H, containing 1.8% $MgSO_4$ and 1.8% $MgSO_4$ plus 1.8% Na_2SO_4, respectively. After storage for 1 year, the cylinders stored in these solutions had begun to show severe distress, indicated by formation of a mushy grey-white material on the surface of the cylinders. This mush was not evident in cylinders under any other storage conditions.

Cement pastes incorporating 5% limestone showed similar behaviour until 168 days storage, when there was evidence for deterioration in some solutions. Whereas storage in water appeared to be benign, storage in magnesium sulfate solutions caused surface crazing and even spalling of surface material. Sodium sulfate solutions appeared to be less aggressive, but there was evidence of spalling between the ages of 168 and 252 days, especially at the higher con-

Table 3
Cement pastes stored in 1.8% $MgSO_4$ + 1.8% Na_2SO_4 solution at 5°C

	Limestone additions (%)			
Age (days)	0	5	15	35
28	White powdery coating No visible deterioration	White powdery coating No visible deteriorato n	White powdery coating No visible deterioration	White powdery coating No visible deterioration
168	White powdery coating No visible deterioration	Crazing of surface Beginning to spall	Expansion, cracking, and spalling	Expansion, cracking, and spalling
336	White powdery coating No cracking but some corrosion at edges	Cracking and spalling Expansion	Expansion, cracking, and extensive spalling	Surface softening and spalling Blisters containing grey-white mush
420	Beginning to crack	Expansion, cracking, and spalling	Partial disintegration Cracking and spalling	Disintegration Spalling and softening

centration used. After storage for 1 year there was evidence of cracking, blistering and expansion.

Cylinders made with cement incorporating 15% limestone showed little or no deterioration until 168 days, when those in several of the solutions began to show signs of cracking and spalling. After storage for 252 days, all of the cylinders were showing signs of distress, even those stored in water. The pastes stored in the solutions containing a high concentration of magnesium sulfate began to show extreme distress, which increased on further storage. These cylinders suffered from extended cracking and severe expansion. After 1 year they had lost their entire outer shells and continued to spall. In solution H (1.8% $MgSO_4$ + 1.8% Na_2SO_4) the outer surfaces of what remained of the original cylinders had become a soft grey-white material.

The incorporation of 35% limestone to the Portland cement paste was particularly deleterious, except for those cylinders stored in water. There was evidence of spalling and cracking from the age of 168 days in all the cylinders stored in solutions containing magnesium sulfate and in the stronger sodium sulfate solution. After 252 days, most of the cylinders had cracked regardless of storage conditions. Those stored in magnesium sulfate solutions showed extensive spalling, cracking, and expansion. By the age of 1 year, the cylinders stored in solutions D and H had almost completely disintegrated to a grey mush in the bottom of the test tube.

It is clear that storage in solution H, containing 1.8% $MgSO_4$ and 1.8% Na_2SO_4, caused the most extensive attack on the cylinders. The behaviour of these cylinders up to 420 days is summarised in Table 3. It can be seen that the extent of the corrosive attack increased with increasing time and with increasing incorporation of limestone. By the end of the storage period, cylinders containing 15 and 35% limestone had severely deteriorated.

3.2. Mineralogy

Changes in mineralogy with continued exposure to sulfate-containing solutions were monitored by XRD, backed up on selected samples by DSC, and also occasionally by differential thermal analysis and infrared spectroscopy, although no results are presented here from these latter methods. Generally, XRD gave a clear indication of the crystalline phases present and results from the other techniques could be interpreted as providing confirmation of this interpretation.

Because ettringite and thaumasite have similar crystal structures [2], their XRD patterns show similarities, as can be seen from Fig. 1. In particular, the two major peaks, at around 9.1 and 16.0° 2θ, are present in both minerals. Although there are small differences in the d-spacings of these peaks in the two minerals, it can be difficult to distinguish them when only small amounts are present, particularly if both may be present in a sample. In most instances, however, sufficient smaller peaks are evident that anyone skilled in the art of XRD can readily identify the presence of either ettringite or thaumasite. In particular, the thaumasite peaks at around 19.5, 23.4, 26.0, and 28.0° 2θ are absent from the ettringite pattern. Likewise, there are prominent ettringite peaks that have no equivalent in the thaumasite pattern (e.g., at 22.9° 2θ).

The thaumasite pattern shown in Fig. 1 matches the standard data (JCPDS file 25-128) very closely and contains no unaccounted peaks. The ettringite pattern similarly is in good agreement with JCPDS file 31-251, but has one additional weak peak at d = 4.89Å, labelled "AH," which is attributed to gibbsite (AH_3, peak at 4.85Å according to JCPDS 29-41). This peak might be due to portlandite, CH, which has a peak at 4.90Å, but gibbsite was thought more likely as it was a reactant in the formation of the standard sample of ettringite.

It was stated above that cylinders made up with cements containing 35% limestone replacement and stored in 1.8% $MgSO_4$ + 1.8% Na_2SO_4 deteriorated after several months. Indeed some such cylinders developed blisters of white material after storage for 196 days. The soft white blister material could be readily separated from the sound unexpanded part of the cylinder and both parts were analysed by XRD as shown in Fig. 2. The mineralogy of the sound part of the cylinder corresponded with that of a normal hydrated Portland cement paste containing calcium hydroxide, ettringite, and a small amount of gypsum, along with a large amount of calcite (because of the limestone incorporation). Small

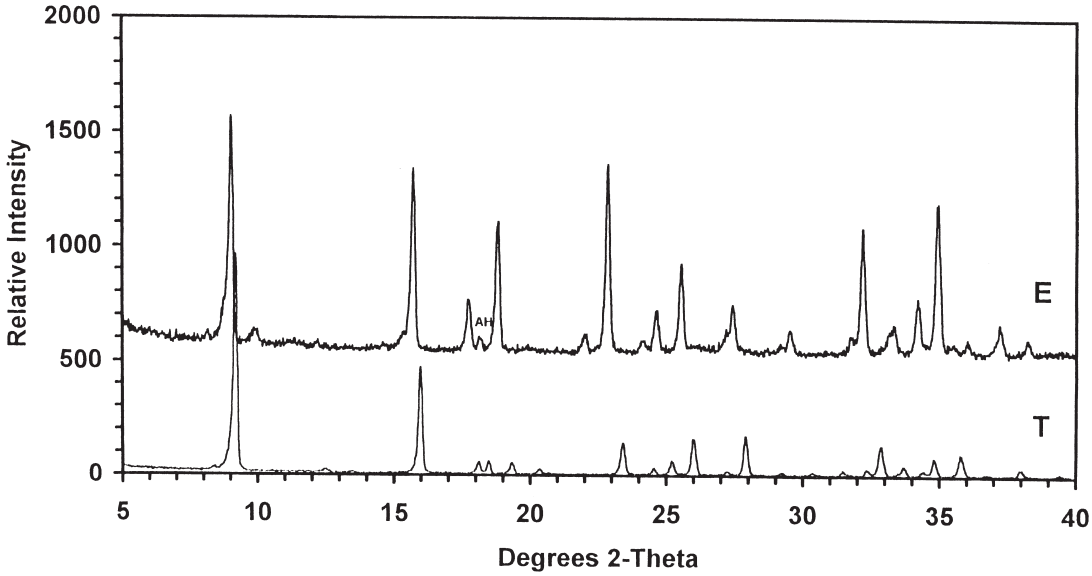

Fig. 1. XRD of ettringite and thaumasite.

amounts of unreacted alite and belite may be present as indicated by the broad peaks between 30 and 35° 2θ. In contrast, the blister material contained thaumasite in place of ettringite, along with a marked reduction in calcium hydroxide (at 18.1 and 34.1° 2θ). Weak peaks at 18.6 and 38.0° 2θ indicated the presence of some brucite, $Mg(OH)_2$. The separation of the thaumasite and ettringite seemed to be almost total, with the XRD pattern from the expanded part of the cylinder including many peaks in excellent agreement with those of the thaumasite standard. Calcite was present in both samples.

These observations are well supported by the evidence obtained from DSC curves of the two parts of the sample, as shown in Figs. 3 and 4. The curves are clearly different, but readily interpreted in the light of the XRD results. The broad endothermic peak between 60 and 140°C in Fig. 3 can be attributed to the presence of ettringite, gypsum, and calcium silicate hydrate gel (not observed by XRD because of its amorphous nature). The strong endothermic peak at 420°C is due to the dehydroxylation of portlandite and indicates the presence of calcium hydroxide as a major hydration product. In Fig. 4 the strong endothermic peak at 115°C is very similar to that obtained from the thaumasite standard, but the standard gave the peak at a higher temperature (136°C). Thermal analysis peak temperatures vary according to the apparatus used and the amount of the phase present. A larger sample examined by DTA gave an endo-

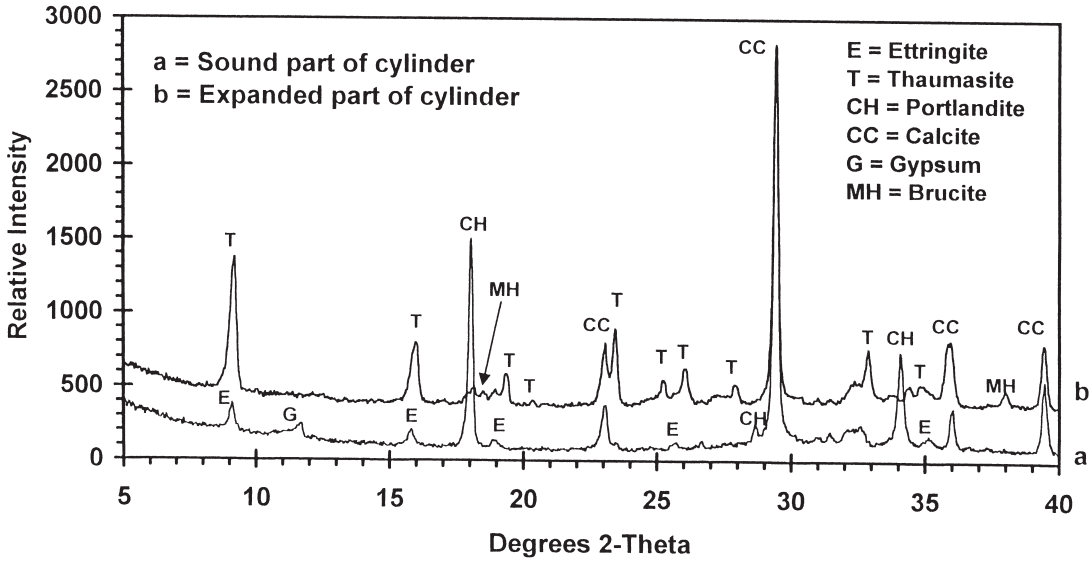

Fig. 2. XRD of OPC-35% limestone paste stored in 1.8% $MgSO_4$ + 1.8% Na_2SO_4 for 196 days. Pattern (a), sound part of cylinder; pattern (b), expanded blister material.

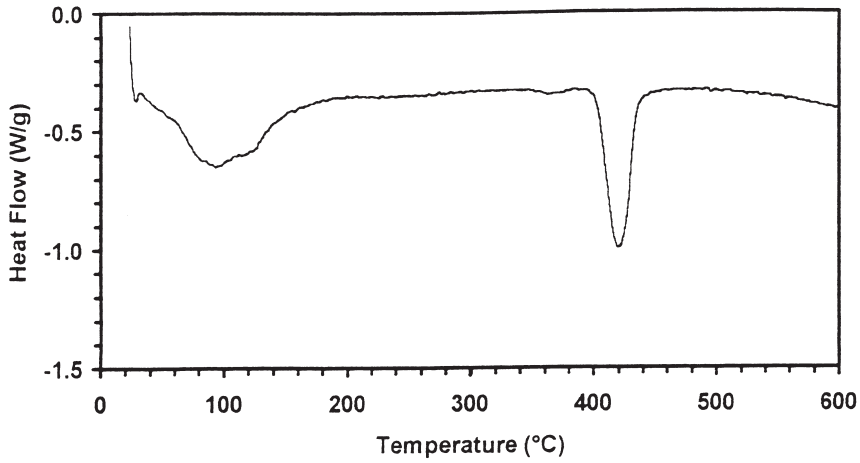

Fig. 3. DSC curve for the sound part of the OPC-35% limestone paste stored in 1.8% $MgSO_4$ + 1.8% Na_2SO_4 at 5°C for 196 days.

thermic peak at 150°C, in close agreement with the curve shown by Bensted and Varma [3]. There is no evidence for a peak due to the presence of calcium hydroxide, but instead a weak endotherm observed at 373°C is attributed to the dehydroxylation of brucite. An even weaker peak at 362°C shown in Fig. 3 may indicate that brucite was also present in trace amounts in the sound part of the cylinder.

Cylinders of OPC 35% limestone stored in 1.8% $MgSO_4$ solution for 280 days had expanded and spalled. The spalled material was shown by XRD (Fig. 5, pattern 1) to contain thaumasite and brucite as well as calcite, but with almost no portlandite present. The remaining corroded cylinder, which was quite firm and still strong, contained ettringite, gypsum, portlandite, and calcite (Fig. 5, pattern 2). The dramatic change in the amount of portlandite present in the two samples can be seen from the relative intensities of the peaks at 18.1 and 34.1° 2θ. Similarly, close inspection of the XRD curves indicates an almost total separation of ettringite and thaumasite in the two samples. In some samples weak peaks due to the presence of monosulfate (AFm) were observed.

It is concluded that thaumasite can be readily formed at 5°C in Portland cement pastes incorporating 35% limestone. The question of whether it can be formed in the presence of much lower levels of replacement arises. The XRD patterns shown in Fig. 6 relate to the hydration products from a paste containing 5% limestone that had been stored in 1.8% $MgSO_4$ + 1.8% Na_2SO_4 solution at 5°C for 336 days (curve b) compared with those from a neat OPC paste stored in water for 28 days (curve a). The crystalline products evident in curve (a) were ettringite, portlandite, and calcite (weak), with major peaks at 9.1, 18.1, and 29.4° 2θ, respectively. Some residual alite and belite may also be present (see peaks between 30 and 35° 2θ), but the peaks are small, broad, and indistinct, making positive identification difficult. There is no evidence for the presence of any gypsum.

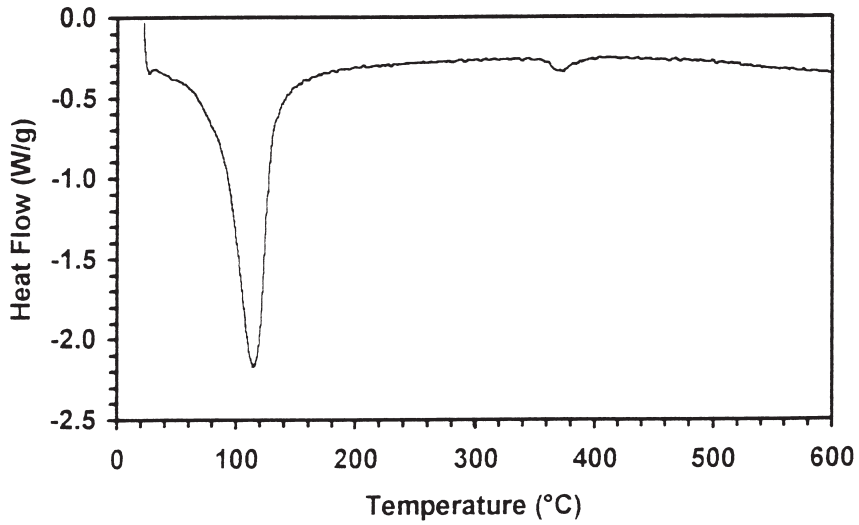

Fig. 4. DSC curve for the expanded part of the OPC-35% limestone paste stored in 1.8% $MgSO_4$ + 1.8% Na_2SO_4 at 5°C for 196 days.

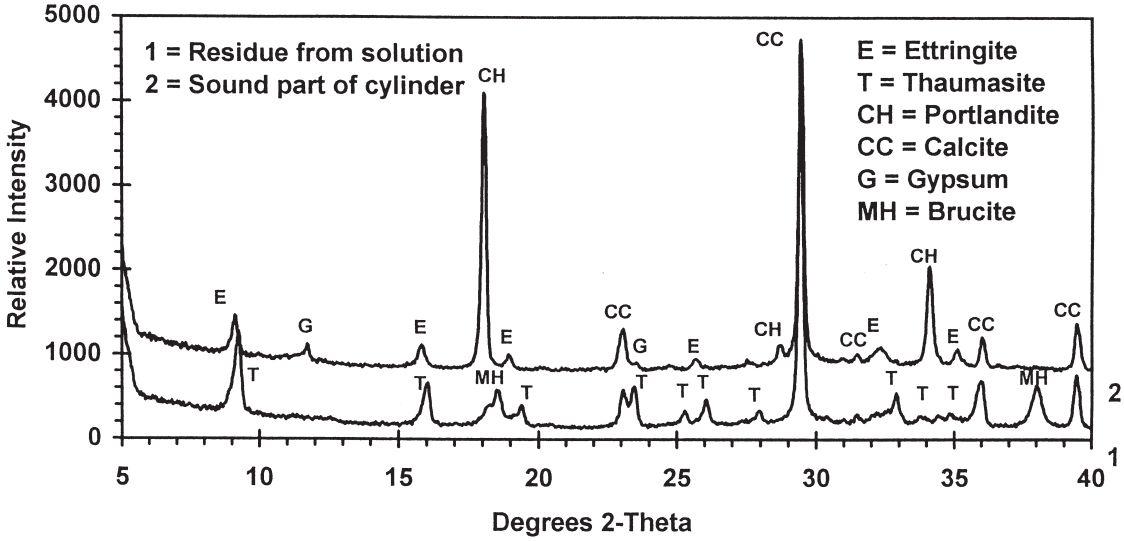

Fig. 5. XRD of OPC-35% limestone paste stored in 1.8% $MgSO_4$ for 280 days. Pattern 1, residue from solution; pattern 2, sound part of the cylinder.

The same phases were observed in curve (b) in the paste containing 5% limestone replacement stored in the stronger mixed sulfate solution. Gypsum was also observed and evidence was obtained for the presence of thaumasite as well as ettringite (note the double peaks at around 9, 16, 27–28, and 32–33° 2θ). Similar XRD patterns were obtained after storage for 280, 308, and 364 days, confirming that small amounts of thaumasite had been formed in the presence of only 5% limestone. The amount of thaumasite formed in the pastes containing 5% limestone was substantially less than in the pastes containing 35% limestone.

In the cement pastes incorporating 15% limestone, evidence for the presence of small amounts of thaumasite, which increased slowly with time, was observed in XRD patterns obtained after 196, 224, 252, 280, 308, 336, and 364 days. More thaumasite was observed in the 15% limestone pastes than in those with only 5% limestone. It was accompanied by ettringite, gypsum, portlandite, and calcite.

Overall samples stored in the stronger magnesium sulfate solution or the stronger mixed sulfate solution were more likely to contain significant amounts of thaumasite than those stored in sodium sulfate or water. The first appearance of thaumasite was generally, although not always, earlier in pastes containing more limestone. Thaumasite formed most readily in pastes containing 35% limestone, but was observed even in pastes containing only 5% limestone.

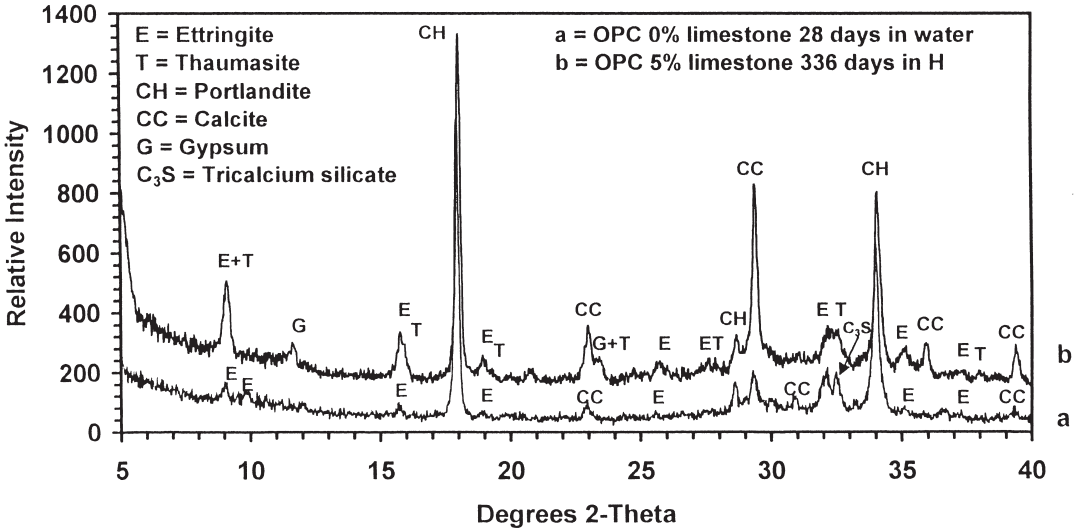

Fig. 6. XRD of OPC-5% limestone paste stored in 1.8% $MgSO_4$ + 1.8% Na_2SO_4 solution at 5°C for 336 days, compared with neat OPC paste stored in water for 28 days.

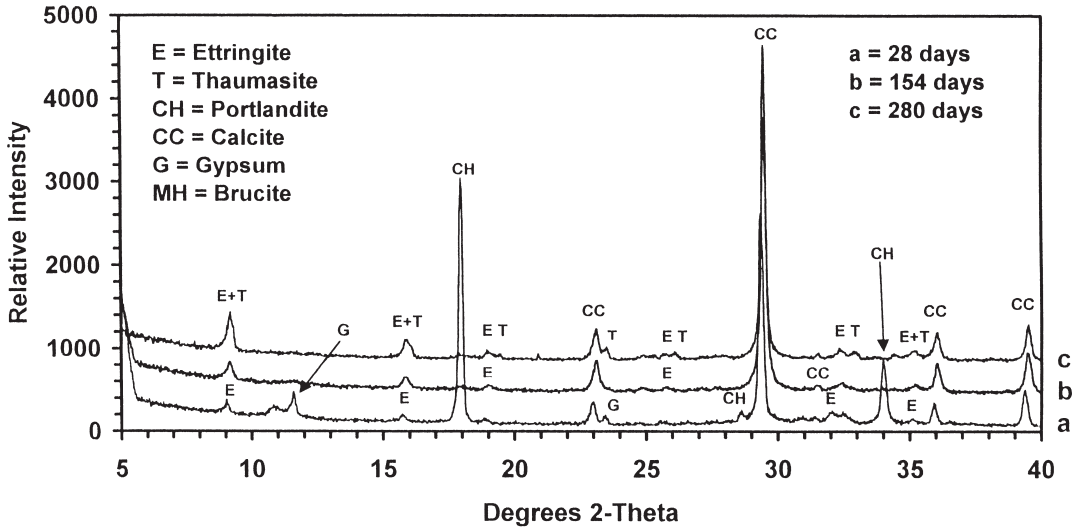

Fig. 7. XRD of OPC-35% limestone paste following cyclic storage in air at room temperature and in 1.8% $MgSO_4$ + 1.8% Na_2SO_4 at 5°C. Curve (a), 28 days; curve (b), 154 days; curve (c), 280 days.

3.3. Effect of alternate wetting and drying

Cylinders of OPC 35% limestone with a water:solids ratio of 0.75 were stored alternately in air at room temperature (about 20°C) and in 1.8% $MgSO_4$ + 1.8% Na_2SO_4 solution at 5°C, following an initial 28 days period of curing in water at room temperature. This cycle was continued for 280 days and X-ray patterns were obtained at 28-day intervals. Three of these patterns are shown in Fig. 7. After 28 days, the expected hydration products of OPC were readily identified, namely portlandite and ettringite with unreacted gypsum, along with strong peaks due to calcite from the limestone replacement. Subsequently, the gypsum and portlandite peaks decreased (and possibly disappeared), while those at 9.1 and 16.0° 2θ increased and broadened. Clear evidence for the formation of small amounts of thaumasite was observed after 280 days.

The surface of the cylinders cracked and spalled and one such sample was examined by SEM after 252 days. At low magnification the surface was observed to be covered with small (<10 μm) subhedral crystals interspersed with finer material. Further examination of the same specimen at higher magnification, shown in Fig. 8, illustrates the morphology of these crystals and their relationship to the finer clusters of short acicular crystals. The needles growing into the cavity were approximately 7 μm long and were arranged randomly, forming a compact mesh. Energy dispersive spectroscopic analysis gave peaks for only calcium and sulfur from the larger crystals, indicating that these were gypsum. Energy dispersive spectroscopic analysis of the finer material indicated the presence of calcium, aluminum, silicon, and sulfur, suggesting an intimate mixture of thaumasite and ettringite, in support of the XRD pattern of the sample that had indicated the presence of both phases.

4. Discussion

From the observations reported in Table 1, it is evident that storage of OPC limestone cement pastes in solutions containing 1.8% $MgSO_4$ brought about severe deterioration after 9 months or longer. Cylinders containing 35% limestone replacement fared worse than those containing 15% limestone, which in turn fared worse than those containing 5% limestone.

In general, the deleterious effects of storage in water were negligible. Storage in magnesium sulfate solutions was more detrimental than storage in sodium sulfate solution. Storage in a mixed solution, containing double the concentration of sulfate ions with respect to the magnesium sulfate solutions, behaved in a similar manner to simple magnesium sulfate solution. This suggests that Mg^{2+} ions play a considerable part in the so-called “sulfate attack” of cements and concretes. This is not a new concept; indeed, Taylor [4] has described a mechanism for “magnesium sulfate attack”.

The relative aggressiveness of the solutions used in this study is outlined below, from least aggressive to most aggressive:

Tap water/distilled water

0.4% Na_2SO_4

1.8% Na_2SO_4

0.4% $MgSO_4$/(0.4% $MgSO_4$ + 0.4% Na_2SO_4)

(1.8% $MgSO_4$ + 1.8% Na_2SO_4)/1.8% $MgSO_4$

Mineralogical characterization, based on XRD backed up by DSC, indicated that a definite reaction sequence was followed. Initially hydration of the Portland cement present led to the formation of calcium silicate hydrate gel (not observed by XRD),

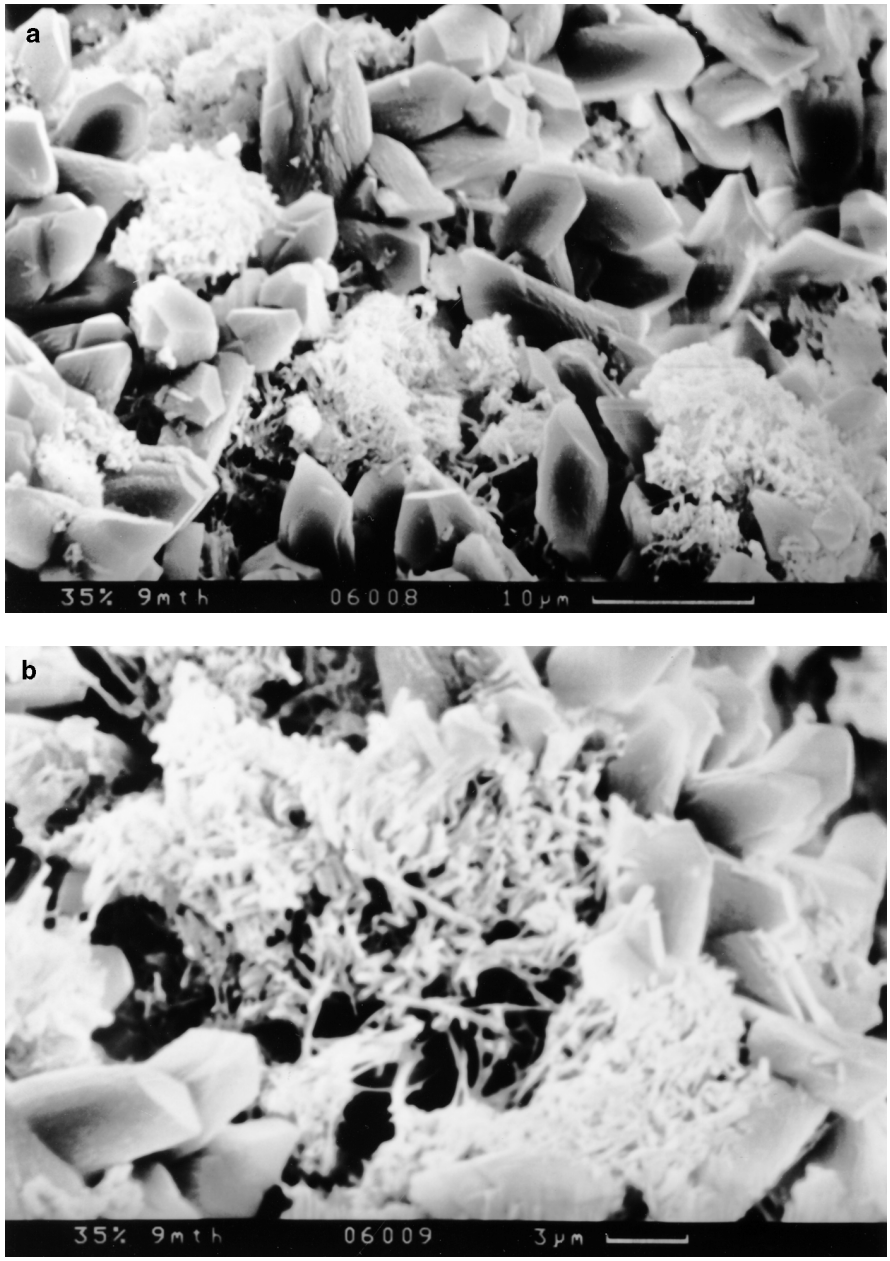

Fig. 8. (a) Secondary electron image of an OPC-35% limestone paste after cyclic storage (see text) for 252 days. (b) The same paste at higher magnification.

portlandite, and ettringite, in the presence of gypsum and calcite (formed in small amounts via carbonation of portlandite in neat cement pastes and present in greater amounts in the OPC limestone pastes). These products are largely due to the reactions of C_3S and C_3A, although the belite and ferrite phases also contribute. The principal reactions are shown in Eq. (1) and Eq. (2):

$$2C_3S + 6H \rightarrow C_3S_2H_3 + 3CH \quad (1)$$

$$C_3A + 3C\bar{S}H_2 + 26H \rightarrow C_6A\bar{S}_3H_{32} \quad (2)$$

In Eq. (1), an approximate formula for C-S-H gel has been assumed to permit the writing of a definite equation, indicating the formation of three moles of portlandite from two moles of C_3S. Calcite is formed in the hydrated cement paste as a result of the reaction between atmospheric carbon dioxide and portlandite as shown in Eq. (3):

$$CH + \bar{C} \rightarrow C\bar{C} + H \quad (3)$$

Eq. (2) shows the formation of ettringite, which continued to form until all the gypsum was consumed. Beyond 56 days in the neat cement paste, small amounts of monosulfate were observed as a result of Eq. (4):

$$2C_3A + C_6A\bar{S}_3H_{32} + 4H \rightarrow 3C_4A\bar{S}H_{12} \quad (4)$$

This conversion is normal in Portland cement pastes because ettringite becomes unstable in the absence of sulfate

ions [4]. The presence of monosulfate in the pastes studied in the present investigation was variable, depending upon the concentration of sulfate ions in solution (N.B. the solutions were renewed every 84 days).

In the case of the neat OPC paste stored in sulfate-containing solutions, gypsum began to crystallize after about 200 days. The formation of this secondary gypsum marked the beginning of obvious sulfate attack, as could be determined from the XRD results. The equations for the formation of secondary gypsum in the presence of sodium sulfate and magnesium sulfate are shown in Eq. (5) and Eq. (6)

$$CH + N\bar{S} + 2H \rightarrow C\bar{S}H_2 + NH \quad (5)$$

$$CH + M\bar{S} + 2H \rightarrow C\bar{S}H_2 + MH \quad (6)$$

The low solubility of magnesium hydroxide provides an impetus for Eq. (6) to proceed and it is accompanied by a drop in pH. In the case of the neat OPC paste, gypsum and ettringite were the only products of sulfate attack and there was no evidence for the formation of thaumasite.

In the presence of fine limestone, thaumasite was detected by XRD after 280 days (with 5% replacement) and after 196 days (with 15% and 30% replacement) in solutions containing 1.8% $MgSO_4$. The delay in the formation of thaumasite seems to have been associated with the reaction of C_3A to form ettringite. Only when all (or nearly all) the C_3A has reacted can thaumasite be formed, accompanied by the formation of brucite in the presence of magnesium sulfate solutions. It is also apparent (from the data shown in Figs. 2, 4, and 5) that calcium hydroxide is a reactant rather than a product during the formation of thaumasite. Hence the "obvious" reaction to form thaumasite, as shown in Eq. (7),

$$C_3S + C\bar{C} + M\bar{S} + 17H \rightarrow C_3S\bar{C}\bar{S}H_{15} + MH + CH \quad (7)$$

is wrong since it shows portlandite as a reaction product.

The experimental evidence presented here conclusively demonstrates that the "delayed" thaumasite formation is from the reaction of C-S-H gel and CH, already produced by the hydration of alite, with carbonate ions from the added limestone and sulfate ions from the external solution, particularly when magnesium is also present. The reaction may be summarised as shown in Eq. (8)

$$C_3S_2H_3 + CH + 2C\bar{C} + 2M\bar{S} + 28H \rightarrow 2C_3S\bar{C}\bar{S}H_{15} + 2MH \quad (8)$$

leading to the formation of brucite in addition to thaumasite, as identified from the XRD and DSC data presented in Figs. 2 through 7.

It has already been pointed out that the hydration of C_3S leads to the formation of one mole of $C_3S_2H_3$ and approximately three moles of CH, according to the actual composition of the C-S-H gel formed. When Eq. (6) is combined with Eq. (8), the overall equation for sulfate attack in the presence of fine limestone additions is seen to be Eq. (9):

$$C_3S_2H_3 + 3CH + 2CC + 4MS + 32H \rightarrow 2C_3S\bar{C}\bar{S}H_{15} + 2C\bar{S}H_2 + 4MH \quad (9)$$

Eq. (9) not only explains the co-formation of secondary gypsum, thaumasite, and brucite, it also predicts that much of the C-S-H gel and portlandite formed from the initial hydration of alite may eventually be consumed. These observations are in agreement with the results observed by visual examination and XRD, and are supported by those from DSC and SEM. The crystalline nature of the secondary gypsum is in accordance with a through solution reaction mechanism and the volume expansion, causing cracking and spalling of the cylinders, may be associated with Eq. (6). There is in fact some evidence (e.g., Fig. 2) to suggest that the secondary gypsum may move ahead of the brucite, sometimes leaving gypsum associated with ettringite in the sound part of the cylinder, while the thaumasite and brucite are discarded in the mush that spalls away because of the expansive forces generated by the chemical reactions. In some field studies that have focused on examination of the "sound" part of the structure that remains, it is possible that the formation of thaumasite and brucite may have been overlooked, leading to the conclusion that conventional sulfate attack had taken place.

The relative proportions by weight of thaumasite:gypsum: brucite predicted by Eq. (9) are 69.8:17.1:13.1, which explains why the observed XRD peaks due to brucite were always weak.

The enhanced sulfate attack in the presence of magnesium ions, provided by $MgSO_4$ solution in the present study, but by dolomite, $CaMg(CO_3)_2$, in some field studies such as those by Bickley et al. [5,6], is due to the very low solubility of magnesium hydroxide. As this phase is formed and precipitates, Eq. (6) is driven to the right-hand side. More secondary gypsum is formed, accompanied by a reduction in the pH as portlandite is consumed. This reduced pH may favour the attack of the C-S-H gel, allowing Eq. (8) to proceed by a through solution mechanism. The overall result is then summarised by the reaction shown in Eq. (9).

Field studies [5–14] have indicated the formation of thaumasite as a degradation product of Portland cement in sulfate environments. In spite of these reports, until recently thaumasite has been regarded as a phase that forms only under exceptional circumstances and it has received relatively little attention. It is shown above that it might indeed be more common than previously suspected, but its formation may have been confused with conventional sulfate attack involving conversion of AFm phases into ettringite in the presence of gypsum. Recent laboratory studies have been relatively few, with the notable exceptions of Crammond and Halliwell [15] and Gaze [16] at the Building Research Establishment. The observations made in the present study are in good agreement with these previous studies.

5. Conclusions

Cement pastes containing fine limestone additions are susceptible to thaumasite formation at 5°C after only a few months of exposure to sulfate solutions. The extent of thau-

masite formation is greater with increasing limestone additions, but some thaumasite is formed in Portland cement containing only 5% fine limestone filler. Corrosive attack is particularly deleterious when magnesium ions are also present; then thaumasite formation is accompanied by formation of brucite and secondary gypsum.

There is always a delay before thaumasite is formed. During this initial period the usual cement hydration reactions take place, leading to the formation of ettringite, C-S-H gel, and portlandite. When all (or nearly all) the C_3A has reacted, the external sulfate supply brings about further chemical reactions. These reactions are not with anhydrous alite, but rather with the products of its hydration. Both C-S-H gel and portlandite are consumed in the process. Calcium hydroxide is a reactant rather than a reaction product. The initial reaction may be that shown previously in Eq. (6). This reaction has several consequences, including the lowering in the pH of the system, perhaps making the C-S-H more vulnerable to chemical attack, and resulting in expansive volume changes that may lead to spalling of the cylinder (or, in the field, of the concrete structure). The overall reaction can be summarised as previously shown in Eq. (9).

Acknowledgments

We should like to thank Dr. N. Crammond and Dr. C.D. Lawrence for helpful discussions. We are grateful to the British Cement Association and the Centre for Cement and Concrete of the University of Sheffield for providing scholarships to S.A. Hartshorn during her period of study and to Mr. P. Livesey of Castle Cement for supplying the Portland cement and limestone filler used in this study.

References

[1] Thaumasite Expert Group, The thaumasite form of sulfate attack: Risks, diagnosis, remedial works and guidance on new construction, Report of the Thaumasite Expert Group, Department of the Environment, Transport and the Regions: London, January, 1999.

[2] R.A. Edge, H.F.W. Taylor, Crystal structure of thaumasite, $[Ca_3Si(OH)_6 \cdot 12H_2O](SO_4)(CO_3)$, Acta Cryst B27 (1971) 594–601.

[3] J. Bensted, S.P. Varma, Studies of thaumasite—Part II, Silicates Ind 39 (1974) 11–19.

[4] H.F.W. Taylor, Cement Chemistry, 2d ed., Thomas Telford Publishing, London, 1997.

[5] J.A. Bickley, R.T. Hemmings, R.D. Hooton, J. Balinsky, Low temperature sulphate attack on Arctic concrete structures: A case history, Proc. 3d Canadian Symp. Cem. and Concr., Ottowa, 1993, pp. 57–117.

[6] J.A. Bickley, R.T. Hemmings, R.D. Hooton, J. Balinsky, Thaumasite related deterioration of concrete structures, Proc. Malhotra Symp. Concr. Technol., San Francisco, 1994, pp. 159–175.

[7] B. Erlin, D.C. Stark, Identification and occurrence of thaumasite in concrete, Highway Res Rec 113 (1966) 108–113.

[8] J.H.P. van Aardt, S. Visser, Thaumasite formation: A cause of deterioration of Portland cement and related substances in the presence of sulphates, Cem Concr Res 5 (1975) 225–232.

[9] M. Regourd, P. Bissery, G. Evers, H. Hornain, B. Mortureux, Ettringite et thaumasite dans le mortier de la digue du port de Cherbourg, Annales ITBTP 358 (1978) 2–14.

[10] R. Lachaud, Thaumasite and ettringite in building materials, Annales ITBTP 370 (1979) 2–7.

[11] R.E. Oberholster, J.H.P. van Aardt, M.P. Brandt, Durability of cementitious systems, in: P. Barnes (Ed.), Structure and Performance of Cements, Applied Science Publishers, London, 1983, pp. 365–413.

[12] R.E. Oberholster, P. Du Toit, J.L. Pretoius, Deterioration of concrete containing a carbonaceous sulphide-bearing aggregate, in: J. Bayles (Ed.), Proc. 6th Intl. Conf. Cem. Microscopy, New Mexico, 1984, pp. 360–373.

[13] N.J. Crammond, Thaumasite in failed cement mortars and renders from exposed brickwork, Cem Concr Res 15 (1985) 1039–1050.

[14] N.J. Crammond, P.J. Nixon, Deterioration of concrete foundation piles as a result of thaumasite formation, in: S. Nagataki (Ed.), Proc. 6th Intl. Conf. Durability Building Materials and Components, E. & F.N. Spon, London, Vol. 1, 1993, pp. 295–305.

[15] N.J. Crammond, M.A. Halliwell, The thaumasite form of sulfate attack in concretes containing a source of carbonate ions—A microstructural overview, in: Advances in Concrete Technology, 2d CANMET/ACI Symp. Adv. Concr. Technol., Las Vegas, 1995, pp. 357–380.

[16] M. Gaze, The effects of varying gypsum content on thaumasite formation in a cement:lime:sand mortar at 5°C, Cem Concr Res 27 (1997) 259–265.